Flow past a circular cylinder (Panton p. 387)

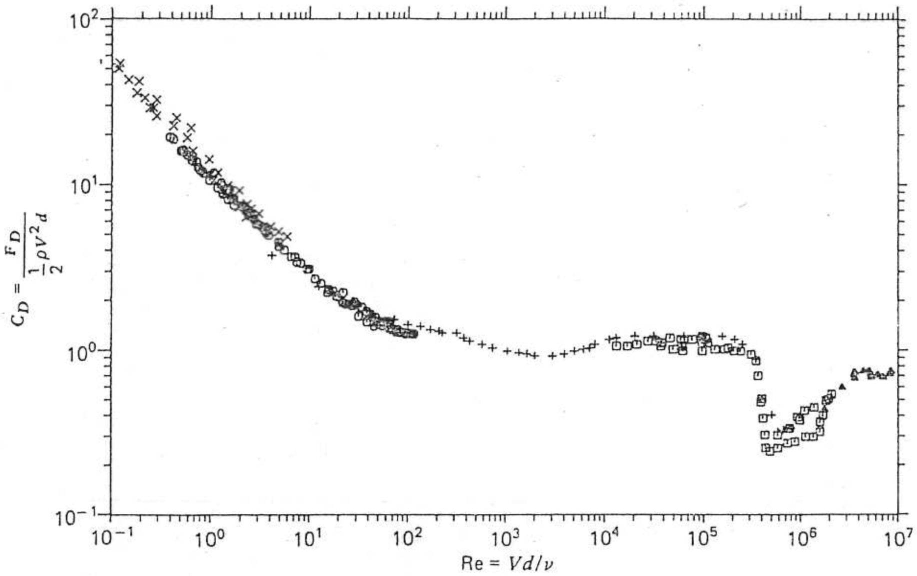

Figure 14.14 Drag curve for a cylinder. Data is from Delany and Sorenson (1953), Finn (1953), Roshko (1961), Tritton (1959), and Wieselsberger (1921).

Data from all kinds of exp. collapses onto the same curve i.e.

$$C_D = f(Re)$$

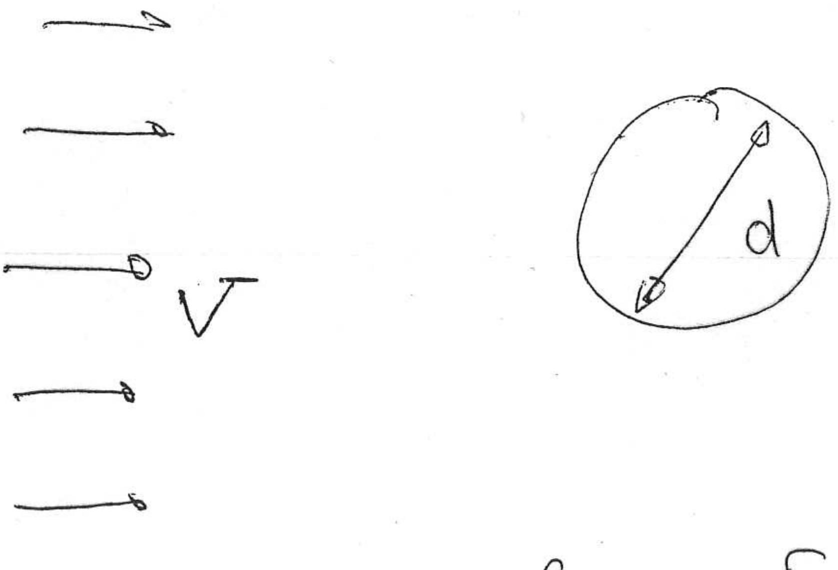

Drag force F_D

$$C_D = \frac{F_D}{\frac{1}{2}\rho V^2 d} \qquad Re = \frac{Vd}{\nu}$$

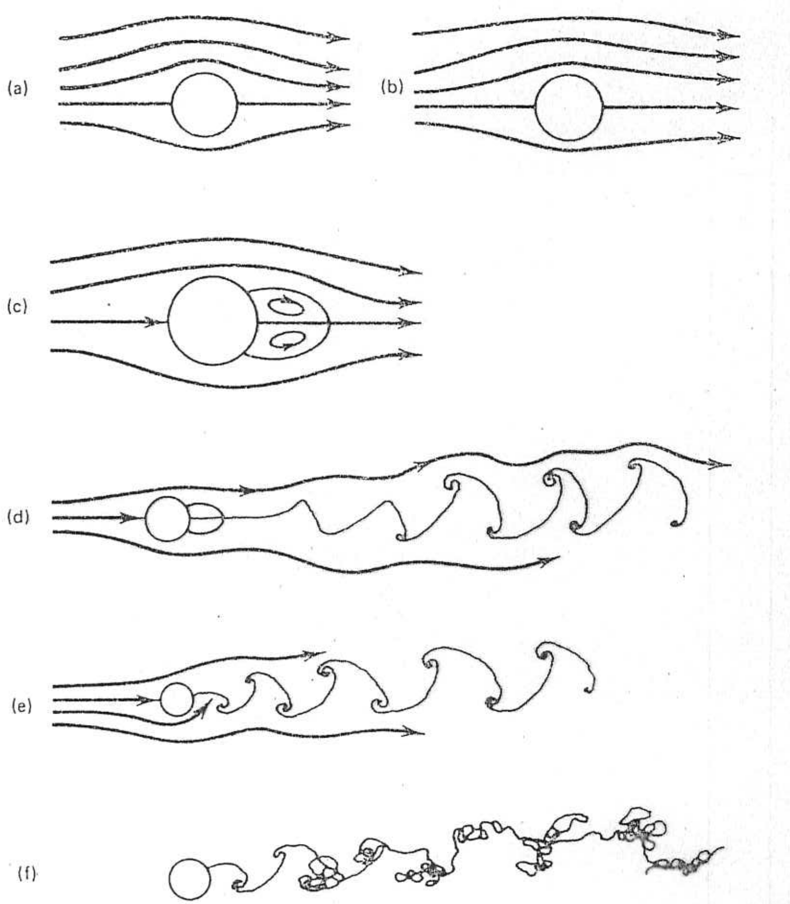

Figure 14.15 Flow regimes for a cylinder: (a) Re = 0, symmetrical; (b) 0 < Re < 4; (c) 4 < Re < 40, attached vortices; (d) 40 < Re < 60–100, von Kármán vortex street; (e) 60–100 < Re < 200, alternate shedding; (f) 200 < Re < 400, vortices unstable to spanwise bending.

then shed. Depending on the details of the experiment, this first occurs at a Reynolds number somewhere between 60 and 100. Figure 14.17a shows the vortex street development. As one goes further downstream the circular motion of the vortices is stopped by viscous forces. In an experiment such as Fig. 14.17 it is difficult to see when this happens as the flow visualization marker retains its distinctive pattern even after the vortices have stopped. The first picture in Fig. 14.18 shows a vortex pattern, the same as in Fig. 14.17, extending a distance of 200 diameters behind the (very small) cylinder. The path line streaks in the figure were produced by smoke from vaporizing oil on a hot wire located at the cylinder station. After some downstream

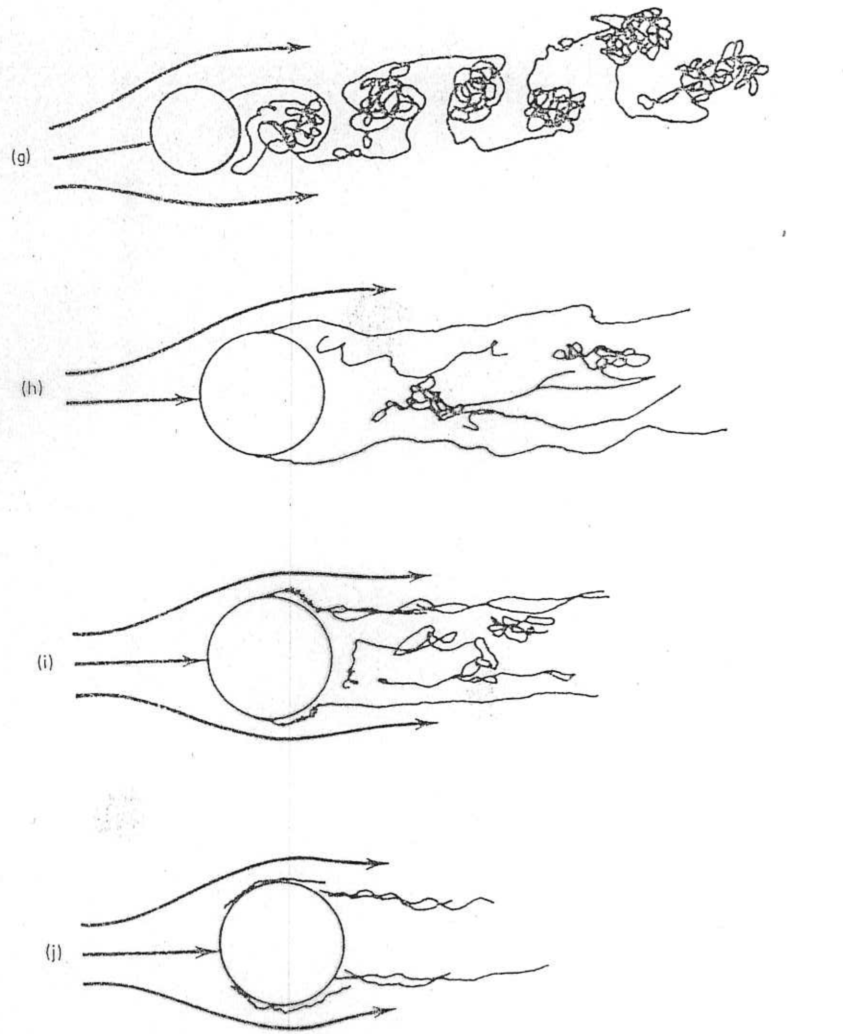

Figure 14.15 (*continued*) (g) 400 < Re, vortices turbulent at birth; (h) Re < 3×10^5, laminar boundary layer separates at 80°; (i) 3×10^5 < Re < 3×10^6, separated region becomes turbulent, reattaches, and separates again at 120°; (j) 3×10^6 < Re, turbulent boundary layer begins on front and separates on back.

a location 150 diameters downstream from the cylinder and no vortices exist. The earlier patterns in the picture in Fig. 14.18a are fossils of events that occur where the smoke was introduced. Cimbala et al. (1988) have not only shown the vortex street decay, but they have also vividly demonstrated how our eyes can be deceived by inactive flow visualization patterns.